

Positronium Formation from Hydrogen Negative Ion, H^-

Puspitapallab Chaudhuri

*Instituto de Física, Universidade de São Paulo,
Caixa Postal 66318, 05315-970 São Paulo, Brazil*

Received on 21 October, 1999. Revised version received on 5 June, 2000.

Theoretical results for the positronium (Ps) formation from hydrogen negative ion, H^- , targets are presented. An exact analytical expression is constructed for the transition matrix for Ps formation in collisions of positrons with H^- in the framework of Born approximation using three different target wave functions. The corresponding differential and total cross sections are presented for Ps formation in ground state. Comparison between these cross sections for different wave functions reveals the dependence of the Ps-formation process on the choice of the target wavefunction and the effect of correlation among the target electrons on the process.

I Introduction

Hydrogen atom, being the simplest system in atomic physics, has been used extensively in the development of quantum mechanics. Despite the repulsive Coulombic interaction between electrons which is equal in magnitude to their attraction to a proton, it is possible to attach an electron to the hydrogen atom. Although very weakly bound, the two electrons and the proton together form the singly charged negative hydrogen ion, H^- . It is the simplest negative ion (bound by a short-range potential).

In last few years, there has been a significant progress in studying collision processes involving H^- . It is of great importance in astrophysics as it plays a fundamental role in maintaining the radiation equilibrium of the solar atmosphere [1] and also provides a stringent test of the approximation methods used in the analysis of two-electron systems [2]. Moreover, H^- also has important biological application as it can be used as an efficient antioxidant in human body [3]. On the other hand, both positron (e^+) and positronium atom (Ps) have different important applications in many different branches of physics. Hence, studying Ps-formation process from H^- by positron impact is something of great interest.

Recently, Lucey et al [4] studied the $(e,2e)$ process on H^- and showed the sensitiveness of the process to the form of the approximation used for the H^- wavefunctions. Quite in the same spirit, we investigate here the positronium formation process by the collision of positron and H^- ($e^+ + H^- \rightarrow Ps + H$) and study the effect of target electron correlation on the formation cross section. In this case the final channel consists of hydrogen atom and the Ps-atom. Both of them are

considered to be in ground state in the present study. We consider three different representations of the H^- wavefunction, correlated and uncorrelated versions of Chandrasekhar representation [5] and Slater representation [2, 4] to calculate the differential and total cross section for the Ps-formation in its ground state. As discussed in the ref. [5] and [4], Chandrasekhar representation which describes one electron as strongly bound and the other loosely bound to the nucleus, gives better ionization potential and ground state energy for H^- . Consideration of the correlation between the electrons improves the energy value considerably. In fact, there exist several different types of H^- wave function. Very recently Le Sech [6] formulated a new correlated version of the H^- wave function which gives slightly better ground state energy than that of Chandrasekhar representation. However, for the time being, we choose to work with Chandrasekhar representation considering the good energy prediction and comparatively simple structure and of the wave function which reduces the computational labour significantly. In table 1 We present the ionization potential and ground state energy of H^- due to various wave functions. The difference between correlated Chandrasekhar representation and Le Sech representation of H^- wave function in terms of the prediction of ground state energy is not much significant and hence, we hope the correlated version of the Chandrasekhar wave function will provide fairly accurate results. Slater wave function for H^- , on the other hand, predicts much higher value of the ground state energy which actually makes H^- an unstable structure [5]. Still we include this in our study as it is interesting to see the effect of wavefunction on the formation process. The two versions of the Chandrasekhar representation will help us to see the effect

of correlation in the Ps-formation from H^- .

Table 1. Ionization potential and ground state energies due to some wavefunctions of H^- compared to the experimental values.

Wavefunction	Ionization potential (a.u.)	Ground State energy (a.u.)
Experimental	0.028	-0.5277
Slater	-0.027	-0.473
Chandrasekhar (Correlated)	0.026	-0.5259
Chandrasekhar (uncorrelated)	0.014	-0.514
Pekeris [7]	0.028	-0.5276
Thakkar & Koga [8]	0.028	-0.5276
Le Sech	0.027	-0.5266
S. H. Patil [9]	0.025	-0.5253

In the present work we use Born approximation (BA) and evaluate the transition matrix in exact analytic form using Lewis integral [10]. Although there exist more refined approximation schemes to estimate scattering parameters, BA still has a significant importance in atomic physics. It gives quite accurate value when the total or partial cross section is not large, as occurs generally at the higher energies [11]. Exact evaluation of the Born scattering amplitude is very important for many of these more refined approximation schemes and useful to have a general view of the corresponding scattering process. Since in the present work we are interested in studying the qualitative behavior of the effect of correlation and the dependence of the scattering cross sections on the choice of wave function, the use BA is sufficient.

We will report the differential and total cross sections for Ps-formation from hydrogen negative ion in a energy range of 50-500 eV using both Chandrasekhar and Slater representation of wavefunction for H^- and compare them among themselves to study the dependence of the process on the choice of target wave function and correlation among target electrons.

II Theoretical development

The three different wave functions of our interest are given by,

i) Slater representation :

$$\psi_{H^-}^{Sl}(\mathbf{r}_i, \mathbf{r}_j) = \frac{Z^3}{\pi} e^{-Z(r_i+r_j)} \quad (1)$$

with $Z = 11/16$.

ii) Chandrasekhar representation :

a) *Uncorrelated version* :

$$\psi_{H^-}^{Uncorr}(\mathbf{r}_i, \mathbf{r}_j) = \frac{N_1}{4\pi} \left(e^{-\alpha r_i - \beta r_j} + e^{-\beta r_i - \alpha r_j} \right) \quad (2)$$

with $N_1 = 0.3948$, $\alpha = 1.039$ and $\beta = 0.283$.

b) *Correlated version* :

$$\psi_{H^-}^{Corr}(\mathbf{r}_i, \mathbf{r}_j) = \frac{N_2}{4\pi} \left(e^{-\alpha r_i - \beta r_j} + e^{-\beta r_i - \alpha r_j} \right) (1 - \mathcal{D}r_{ij}) \quad (3)$$

with $N_2 = 0.36598$, $\alpha = 1.0748$, $\beta = 0.4776$ and $\mathcal{D} = 0.31214$. In this work we shall use $i = 2$ and $j = 3$.

In atomic units, the first Born scattering amplitude for Ps-formation from H^- is given by

$$f^B(\mathbf{k}_f, \mathbf{k}_i) = \frac{1}{\pi} \int \phi^*(\mathbf{r}_3) \omega^*(\mathbf{r}_{12}) e^{-i\mathbf{k}_f \cdot \mathbf{S}_{12}} V(\mathbf{r}_1, \mathbf{r}_2, \mathbf{r}_3) \psi(\mathbf{r}_2, \mathbf{r}_3) e^{i\mathbf{k}_i \cdot \mathbf{r}_1} d\mathbf{r}_1 d\mathbf{r}_2 d\mathbf{r}_3, \quad (4)$$

where

$$V(\mathbf{r}_1, \mathbf{r}_2, \mathbf{r}_3) = \left(\frac{1}{r_1} - \frac{1}{r_2} + \frac{1}{r_{23}} - \frac{1}{r_{13}} \right). \quad (5)$$

For the purpose of studying the initial target-state electron correlation on the final channel we choose the post form of the interaction. In writing (4) we denote the incident positron and two electrons of the target hydrogen negative ion as particles 1, 2 and 3 respectively. Here $\psi(\mathbf{r}_2, \mathbf{r}_3)$, $\phi(\mathbf{r}_3)$ are the wave functions of the target H^- and the neutral hydrogen atom of the final channel in the ground state, respectively and $\omega(\mathbf{r}_{12})$ that of the positronium atom with

$$\mathbf{S}_{12} = \frac{1}{2}(\mathbf{r}_1 + \mathbf{r}_2); \quad \mathbf{r}_{12} = \mathbf{r}_1 - \mathbf{r}_2. \quad (6)$$

\mathbf{S}_{12} stands for the centre-of-mass coordinate of the positronium.

The wave number of the positron, \mathbf{k}_i , and that of the positronium (Ps), \mathbf{k}_f are related through conservation of energy by

$$\frac{1}{2\mu_i}k_i^2 + E_{\text{H}^-} = \frac{1}{2\mu_f}k_f^2 + E_{\text{Ps}} + E_{\text{H}} \quad (7)$$

where E_{H^-} is the ground state energy of the hydrogen negative ion, $E_{\text{Ps}}=-0.25$ a.u. and $E_{\text{H}}=-0.5$ a.u. μ_i and μ_f are the reduced masses in the initial and final channels respectively ($\mu_i=1, \mu_f=2$). Thus the energy conservation relation in the present case becomes,

$$k_i^2 + 2E_{\text{H}^-} = \frac{1}{2}k_f^2 - 1.5 \quad (8)$$

To evaluate the amplitude in (4) we work with the ground state hydrogen wave function, $\frac{1}{\sqrt{\pi}}e^{-r_3}$ and the ground state positronium wave function is taken as $\frac{1}{\sqrt{8\pi}}e^{-\mu r_{12}}|_{\mu=0.5}$. Also we use the Fourier transformation

$$e^{-\mu r_{ij}} = \frac{\mu}{\pi^2} \int \frac{e^{i\mathbf{P}\cdot(\vec{r}_i - \vec{r}_j)}}{(\mu^2 + p^2)^2} d\mathbf{p}. \quad (9)$$

Then the radial equation in (4) become separable and can be arranged in terms of Lewis integral [10] which has standard analytical solution. The final expression of the scattering amplitude for each wave function considered is given below:

i) for Slater representation of the wavefunction, eqn. (1)

$$f^B(\mathbf{k}_f, \mathbf{k}_i) = I_1 + I_2, \quad (10)$$

where

$$I_1 = A - B, \quad (11)$$

$$I_2 = C - D. \quad (12)$$

Now using some general notations, $Q_{mn}(\mu, \zeta_i; x, \mathbf{y})$ and $L_{lmn}(\mu; \zeta_i, \mu_1; \zeta_f, \mu_2)$ (whose definitions will be given later) we can write

$$A = \frac{8\sqrt{8}Z^3}{\pi^2(1+Z)^3} \lim_{t \rightarrow 0} L_{101}(\mu; \zeta_i, t; \zeta_f, Z), \quad (13)$$

$$B = \frac{32\sqrt{8}Z^3\mu}{(1+Z)^3} Q_{21}(\mu, \zeta_i; Z, \mathbf{K}), \quad (14)$$

$$C = \frac{32\sqrt{8}Z^3\mu}{(1+Z)^3} \left[Q_{21}(\mu, \zeta_i; Z, \mathbf{K}) - \{(2Z+1)(Z+1)\} Q_{22}(\mu, \zeta_i; 2Z+1, \mathbf{K}) - Q_{21}(\mu, \zeta_i; 2Z+1, \mathbf{K}) \right], \quad (15)$$

$$D = \frac{8\sqrt{8}Z^3}{\pi^2(1+Z)^3} \left[\lim_{t \rightarrow 0} L_{101}(\mu; \zeta_i, t; \zeta_f, \alpha) - \frac{1}{2}(1+Z)L_{111}(\mu; \zeta_i, 1+Z; \zeta_f, \alpha) - L_{101}(\mu; \zeta_i, 1+Z; \zeta_f, \alpha) \right]. \quad (16)$$

ii) for *uncorrelated* representation of Chandrasekhar wave function, eqn. (2)

$$f^B(\mathbf{k}_f, \mathbf{k}_i) = I_1 + I_2 \quad (17)$$

where

$$I_1 = A + B, \quad (18)$$

$$I_2 = C + D. \quad (19)$$

with

$$A = \frac{64C\pi}{(\beta+1)^3} \lim_{t \rightarrow 0} L_{101}(\mu; \zeta_i, t; \zeta_f, \alpha) - \frac{256C\mu\pi^3}{(\beta+1)^3} Q_{21}(\mu, \zeta_i; \alpha, \mathbf{K}), \quad (20)$$

$$B = \frac{64\mathcal{C}\pi}{(\alpha+1)^3} \lim_{t \rightarrow 0} L_{101}(\mu, \zeta_i, t; \zeta_f, \beta) - \frac{256\mathcal{C}\mu\pi^3}{(\alpha+1)^3} Q_{21}(\mu, \zeta_i; \beta, \mathbf{K}), \quad (21)$$

$$C = i_1^C - i_2^C, \quad (22)$$

with,

$$i_1^C = \frac{256\mathcal{C}\pi^3\mu}{(\beta+1)^3} \left[Q_{21}(\mu, \zeta_i; \alpha, \mathbf{K}) - \{Y(\beta+1)\} Q_{22}(\mu, \zeta_i; Y, \mathbf{K}) - Q_{21}(\mu, \zeta_i; Y, \mathbf{K}) \right], \quad (23)$$

$$i_2^C = \frac{64\mathcal{C}\pi}{(\beta+1)^3} \left[\lim_{t \rightarrow 0} L_{101}(\mu, \zeta_i, t; \zeta_f, \alpha) - \frac{1}{2}(\beta+1)L_{111}(\mu, \zeta_i, \beta+1; \zeta_f, \alpha) - L_{101}(\mu, \zeta_i, \beta+1; \zeta_f, \alpha) \right], \quad (24)$$

and

$$D = i_1^D - i_2^D. \quad (25)$$

with,

$$i_1^D = \frac{256\mathcal{C}\pi^3\mu}{(\alpha+1)^3} \left[Q_{21}(\mu, \zeta_i; \beta, \mathbf{K}) - \{Y(\alpha+1)\} Q_{22}(\mu, \zeta_i; Y, \mathbf{K}) - Q_{21}(\mu, \zeta_i; Y, \mathbf{K}) \right], \quad (26)$$

$$i_2^D = \frac{64\mathcal{C}\pi}{(\alpha+1)^3} \left[\lim_{t \rightarrow 0} L_{101}(\mu, \zeta_i, t; \zeta_f, \beta) - \frac{1}{2}(\alpha+1)L_{111}(\mu, \zeta_i, \alpha+1; \zeta_f, \beta) - L_{101}(\mu, \zeta_i, \alpha+1; \zeta_f, \beta) \right]. \quad (27)$$

In this case $Y = \alpha + \beta + 1$ and $\mathcal{C} = N_1/8\sqrt{2}\pi^3$.

iii) for *correlated* representation of Chandrasekhar wave function, eqn. (3)

$$f^B(\mathbf{k}_f, \mathbf{k}_i) = I_1 + I_2 - I_3, \quad (28)$$

where,

$$I_1 = A + B, \quad (29)$$

$$I_2 = C + D, \quad (30)$$

$$I_3 = E + F. \quad (31)$$

$$A = \frac{64\mathcal{C}\pi}{(\beta+1)^3} \left[-4\mu\pi^2 \left\{ Q_{21}(\mu, \zeta_i; Y, \mathbf{K}) + (1+\beta)YQ_{22}(\mu, \zeta_i; Y, \mathbf{K}) \right\} - \left\{ \frac{(1+\beta)}{2}L_{111}(\mu, \zeta_i, 1+\beta; \zeta_f, \alpha) - L_{101}(\mu, \zeta_i, 1+\beta; \zeta_f, \alpha) \right\} \right] \quad (32)$$

$$B = \frac{64\mathcal{C}\pi}{(\alpha+1)^3} \left[-4\mu\pi^2 \left\{ Q_{21}(\mu, \zeta_i; Y, \mathbf{K}) + (1+\alpha)YQ_{22}(\mu, \zeta_i; Y, \mathbf{K}) \right\} - \left\{ \frac{(1+\alpha)}{2}L_{111}(\mu, \zeta_i, 1+\alpha; \zeta_f, \beta) - L_{101}(\mu, \zeta_i, 1+\alpha; \zeta_f, \beta) \right\} \right] \quad (33)$$

$$C = \frac{64\mathcal{C}\mathcal{D}\pi}{(\beta+1)^3} \left[4\mu\pi^2 \left\{ -4Y^2(1+\beta)Q_{23}(\mu, \zeta_i; Y, \mathbf{K}) + (1+\beta-2Y)Q_{22}(\mu, \zeta_i; Y, \mathbf{K}) \right\} + \left\{ \frac{(1+\beta)}{2}L_{112}(\mu, \zeta_i, 1+\beta; \zeta_f, \alpha) + \frac{(1+\beta)}{2\alpha}L_{111}(\mu, \zeta_i, 1+\beta; \zeta_f, \alpha) - L_{102}(\mu, \zeta_i, 1+\beta; \zeta_f, \alpha) - \frac{1}{\alpha}L_{101}(\mu, \zeta_i, 1+\beta; \zeta_f, \alpha) \right\} \right] \quad (34)$$

$$D = \frac{64\mathcal{C}\mathcal{D}\pi}{(\alpha + 1)^3} \left[4\mu\pi^2 \left\{ -4Y^2(1 + \alpha)Q_{23}(\mu, \zeta_i; Y, \mathbf{K}) + (1 + \alpha - 2Y)Q_{22}(\mu, \zeta_i; Y, \mathbf{K}) \right\} + \left\{ \frac{(1 + \alpha)}{2}L_{112}(\mu; \zeta_i, 1 + \alpha; \zeta_f, \beta) + \frac{(1 + \alpha)}{2\beta}L_{111}(\mu; \zeta_i, 1 + \alpha; \zeta_f, \beta) - L_{102}(\mu; \zeta_i, 1 + \alpha; \zeta_f, \beta) - \frac{1}{\beta}L_{101}(\mu; \zeta_i, 1 + \alpha; \zeta_f, \beta) \right\} \right] \quad (35)$$

$$E = \frac{64\mathcal{C}\mathcal{D}\pi}{(\beta + 1)^4} \left[-4\mu\pi^2 \left\{ 4Y(1 + \beta)^2Q_{23}(\mu, \zeta_i; Y, \mathbf{K}) + (5Y - 1)(1 + \beta)^2Q_{22}(\mu, \zeta_i; Y, \mathbf{K}) + 3Q_{21}(\mu, \zeta_i; Y, \mathbf{K}) - Y(1 + \beta)Q_{22}(\mu, \zeta_i; Y, \mathbf{K}) \right\} + \left\{ \frac{(1 + \beta)^2}{2}L_{121}(\mu; \zeta_i, 1 + \beta; \zeta_f, \alpha) - 1.5(1 + \beta)L_{111}(\mu; \zeta_i, 1 + \beta; \zeta_f, \alpha) + 3L_{101}(\mu; \zeta_i, 1 + \beta; \zeta_f, \alpha) \right\} \right] \quad (36)$$

and

$$F = \frac{64\mathcal{C}\mathcal{D}\pi}{(\alpha + 1)^4} \left[-4\mu\pi^2 \left\{ 4Y(1 + \alpha)^2Q_{23}(\mu, \zeta_i; Y, \mathbf{K}) + (5Y - 1)(1 + \alpha)^2Q_{22}(\mu, \zeta_i; Y, \mathbf{K}) + 3Q_{21}(\mu, \zeta_i; Y, \mathbf{K}) - Y(1 + \alpha)Q_{22}(\mu, \zeta_i; Y, \mathbf{K}) \right\} + \left\{ \frac{(1 + \alpha)^2}{2}L_{121}(\mu; \zeta_i, 1 + \alpha; \zeta_f, \alpha) - 1.5(1 + \alpha)L_{111}(\mu; \zeta_i, 1 + \alpha; \zeta_f, \beta) + 3L_{101}(\mu; \zeta_i, 1 + \alpha; \zeta_f, \beta) \right\} \right] \quad (37)$$

where $Y = \alpha + \beta + 1$, $\mathcal{C} = N_2/8\sqrt{2}\pi^3$ and $\mathcal{D} = 0.31214$.

The mathematical expression of the scattering amplitude thus becomes more and more complex from Slater representation to the correlated version of Chandrasekhar representation. In writing all the expressions above we use a few general notations that are defined below :

$$\zeta_f = \frac{\mathbf{k}_f}{2} \quad \zeta_i = \mathbf{k}_i - \frac{\mathbf{k}_f}{2} \quad \text{and} \quad \mathbf{K} = \mathbf{k}_i - \mathbf{k}_f, \quad (38)$$

$$Q_{mn}(\mu, \zeta_i; x, \mathbf{y}) = \frac{1}{(\mu^2 + \zeta_i^2)^m (x^2 + y^2)^n} \quad (39)$$

and

$$L_{lmn}(\mu; \zeta_i, \mu_1; \zeta_f, \mu_2) = \frac{\partial^l}{\partial \mu^l} \frac{\partial^m}{\partial \mu_1^m} \frac{\partial^n}{\partial \mu_2^n} L_{000}(\mu; \zeta_i, \mu_1; \zeta_f, \mu_2) \quad (40)$$

with

$$L_{000}(\mu, \zeta_i, \mu_1; \zeta_f, \mu_2) = \int \frac{1}{(p^2 + \mu^2)(|\mathbf{p} + \zeta_i|^2 + \mu_1^2)} \frac{1}{(|\mathbf{p} + \zeta_f|^2 + \mu_2^2)} d\mathbf{p}. \quad (41)$$

L_{000} is the Lewis integral [10] that has analytical solution given by,

$$L_{000}(\mu; \mathbf{q}_1, a; \mathbf{q}_2, b) = \int \frac{1}{(p^2 + \mu^2)(|\mathbf{p} - \mathbf{q}_1|^2 + a^2)} \frac{1}{(|\mathbf{p} - \mathbf{q}_2|^2 + b^2)} d\mathbf{p} = \frac{\pi^2}{\xi^{\frac{1}{2}}} \log \left[\frac{(\beta + \xi^{\frac{1}{2}})}{(\beta - \xi^{\frac{1}{2}})} \right], \quad (42)$$

$$\xi = \alpha\gamma - \beta^2 \quad (43)$$

$$\alpha\gamma = \{(\mathbf{q}_1 - \mathbf{q}_2)^2 + (a + b)^2\} q_1^2 + (\mu + a)^2 q_2^2 + (b + \mu)^2 \quad (44)$$

$$\beta = \mu\{(\mathbf{q}_1 - \mathbf{q}_2)^2 + (a + b)^2\} + b\{q_1^2 + (\mu + a)^2\} + a\{q_2^2 + (\mu + b)^2\} - 4ab\mu \quad (45)$$

The generalised Lewis integrals $L_{lmn}(\mu; \zeta_f, \mu_1; \zeta_i, \mu_2)$ of order ≤ 3 (i.e. $l + m + n = 3$) have been evaluated numerically by the procedure of Roy et al [12]. The higher order Lewis integrals are evaluated using its equality with Dalitz integral, $D_{lmn} = L_{lmn}$ [12] where

$$D_{lmn} = \pi^2 \frac{\partial^{m+n}}{\partial \mu_1^m \partial \mu_2^n} \int_0^1 dx \frac{1}{\mu} \frac{\partial}{\partial \mu_0^l} \left[\frac{1}{\omega^2 + \delta^2} \right]. \quad (46)$$

with

$$\omega = x\mathbf{q}_1 + (1-x)\mathbf{q}_2, \quad (47)$$

$$\mu^2 = x\mu_1^2 + (1-x)\mu_2^2 + x(1-x)|\mathbf{q}_1 - \mathbf{q}_2|^2 \quad (48)$$

and

$$\delta = \mu_0 + \mu \quad (49)$$

The Dalitz integrals are carried out by a 16 point Gauss-Legendre quadrature with subsequent division of the interval (0,1) to obtain a pre-determined relative error of 10^{-10} . The total cross sections are calculated numerically by using a Gauss-Legendre quadrature method for integrating the differential cross section over the cosine of the scattering angle.

III Results and discussion

Based on the exact analytic evaluation of the first Born transition matrix we have computed the differential cross sections $(d\sigma/d\Omega)$ and total cross sections (σ) for the positronium formation using the standard definitions [13] with all the three scattering amplitude mentioned in the previous section. For brevity, we denote the differential cross sections due to Slater wave function as $(d\sigma/d\Omega)_{slater}$ and that due to correlated and uncorrelated Chandrasekhar wave function as $(d\sigma/d\Omega)_{corr}$ and $(d\sigma/d\Omega)_{uncorr}$ respectively. In Figs 1 and 2, we present a comparative study of the differential cross sections due to the three wave functions.

In Fig. 1, we plot $(d\sigma/d\Omega)_{slater}$, $(d\sigma/d\Omega)_{corr}$ and $(d\sigma/d\Omega)_{uncorr}$ separately each for three energies, $E=100, 300$ and 500 eV to have a comparison among themselves while in Fig. 2, $(d\sigma/d\Omega)_{slater}$, $(d\sigma/d\Omega)_{corr}$ and $(d\sigma/d\Omega)_{uncorr}$ are compared for incident energies $E=100, 200, 300$ and 400 eV. Qualitatively, each of the curves with uncorrelated wave function has the same feature having a sharp minimum. As energy increases, amplitude due to the repulsive interaction part as well as that due to the attractive part become more and more peaked in the forward direction and the minima move towards the smaller angles. The occurrence of the sharp minima is due to the destructive interference of the attractive and repulsive parts of the interaction potential. However, $(d\sigma/d\Omega)_{uncorr}$ shows a different nature. Unlike the uncorrelated case, the inter-electronic repulsion pushes the dip of the correlated wave-function towards higher scattering angles with the increase of energy and disappears completely after 200 eV. After

that the cross section decreases in a smooth exponential manner. From Fig. 1 we can see that in case of $(d\sigma/d\Omega)_{slater}$, the minima are more or less at the same scattering angle for all energies, the movement being extremely slow. But in case of $(d\sigma/d\Omega)_{uncorr}$ the minima move towards forward scattering angle with the increase of energy at a faster rate. However in both the cases of uncorrelated wave-function the minima are located somewhere around 30° scattering angle.

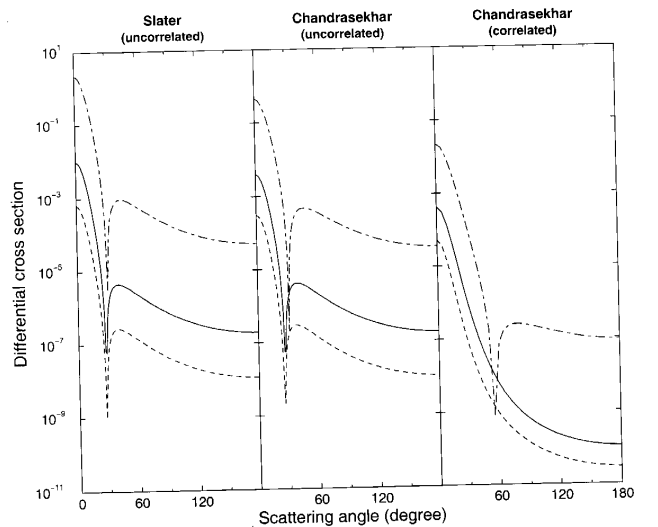


Figure 1. A comparison of differential cross sections (in units of a_0^2) for the formation of Ps(1s) state from H^- using Slater wave function, uncorrelated Chandrasekhar wave function and correlated Chandrasekhar wave function respectively. Each block contains differential cross section curves for incident positron energy $E=100$ eV (dashed-dotted line), $E=300$ eV (dotted line) and $E=500$ eV (Solid line).

In Fig. 2, we compare the differential cross sections for the three wave functions at four particular energies. Here we see, $(d\sigma/d\Omega)_{slater}$ is always a bit higher than $(d\sigma/d\Omega)_{uncorr}$ for scattering angles below 20° and above 30° at all energies, but the difference between them diminishes with the increase of energy. However, comparing with $(d\sigma/d\Omega)_{corr}$ we can say that $(d\sigma/d\Omega)_{slater}$ lies more or less close to $(d\sigma/d\Omega)_{uncorr}$ at all energies in spite of the important fact that Slater wave function provides a poorer value of ground state energy of H^- than that provided by uncorrelated Chandrasekhar wave function (table 1). In this context, its worth noting that $(d\sigma/d\Omega)_{corr}$ runs always lower than $(d\sigma/d\Omega)_{slater}$ and $(d\sigma/d\Omega)_{uncorr}$ and the difference among them is significant. Hence we can conclude that to study the Ps-formation from H^- , consideration of the correlation among the target electrons is very important.

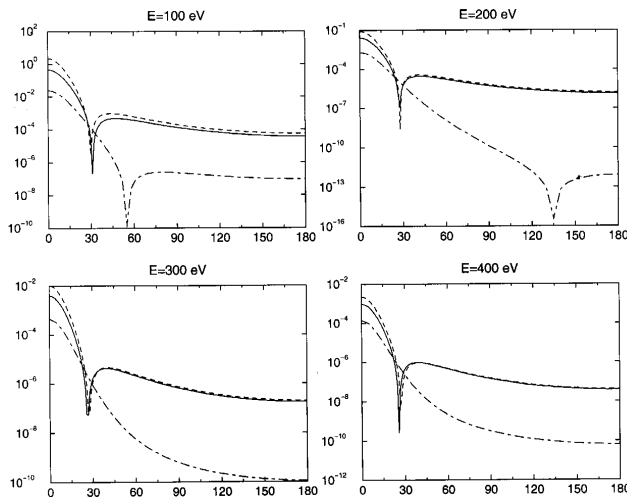


Figure 2. A comparison of differential cross sections (in units of a_0^2) for the formation of Ps(1s) state from H^- using Slater wave function (dotted line), uncorrelated Chandrasekhar wave function (solid line) and correlated Chandrasekhar wave function (dashed-dotted line) respectively at different energies. In the figure, x-axis denotes the scattering angle in degrees while y-axis is the differential cross sections.

In Fig. 3 we display the results for the total cross section for Ps-formation in ground state using the three different representations. Unlike the differential cross sections, total cross sections due to Slater representation are always higher than that of uncorrelated Chandrasekhar representation, however the difference diminishes with increase of energy. This is due to the higher values of the $(d\sigma/d\Omega)_{slater}$ for the lower scattering angles which contribute most to the total cross section values. The total cross section due to correlated Chandrasekhar wave function is much smaller than both the two uncorrelated wave function as expected. Since there exist no experimental results for capture cross sections in $e^+ - H^-$ collisions comparison of our cross sections is not possible.

In conclusion, we have performed an closed analytical calculation of first Born transition matrix element and present the differential and total cross section for positronium formation in ground state in $e^+ - H^-$ collision for different positron impact energies. A comparison between the Slater representation and more accurate Chandrasekhar representations, both in uncorrelated and correlated version, of wave function for hydrogen negative ion has been drawn through these Ps-formation cross section values. It is clear from the comparison that the Ps-formation process from H^- is quite sensitive to the choice of target wave function and the consideration of the correlation effect between the electrons of target H^- is very important. Its beyond doubt that to get more clear picture of the particular process, more refined models and approximations are required which we will consider in our forthcoming studies. However, the present method of analytical calculation will

reduce the computational labour significantly in more advanced studies. Moreover, we believe that the present endeavour will help to provide a general idea about the Ps-formation process from hydrogen negative ion, H^- and a clear visualization of the effect of the electron correlation on this rearrangement process.

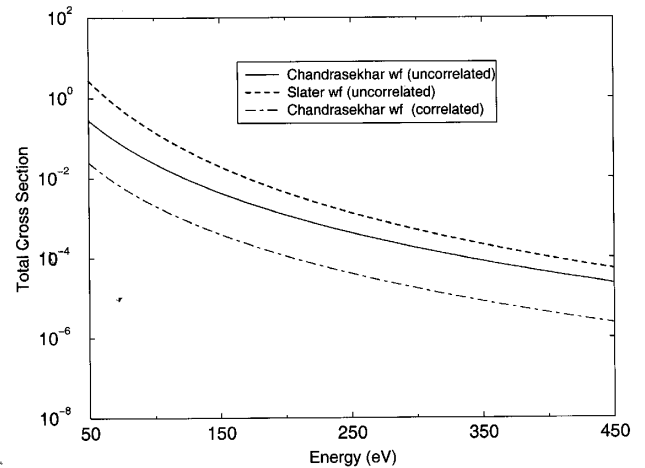


Figure 3. Total cross sections (in units of πa_0^2) for the Ps(1s)-formation from H^- using Slater wave function (dotted line), uncorrelated Chandrasekhar wave function (solid line) and correlated Chandrasekhar wave function (dashed-dotted line) respectively at different energies.

The author would like to thank Prof A. S. Ghosh for useful discussions and FAPESP for the financial support.

References

- [1] S. Chandrasekhar and D. D. Elbert, *Astrophys. J* **128**, 633 (1958).
- [2] B. H. Bransden and C. J. Joachain, *Physics of Atoms and Molecules* (London : Longman, 1983).
- [3] www.nutribiz.com/h_ions.html
- [4] S. Lucey, C. T. Whelan, R. J. Allan and H. R. J. Walters, *J. Phys. B: At. Mol. Phys* **29**, L489 (1996).
- [5] S. Chandrasekhar, *Astrophys. J* **100**, 176 (1945).
- [6] C. L. Sech, *J. Phys. B: At. Mol. Phys* **29**, L47 (1997).
- [7] C. L. Pekeris, *Phys Rev* **115**, 1216 (1959), **126** 1470 (1962).
- [8] A. J. Thakkar and T. Koga, *Phys Rev. A* **50**, 854 (1994).
- [9] S. H. Patil, *Euro. Phys. J. D* **6**, 171 (1999).
- [10] R. R. Lewis, Jr, *Phys Rev* **102**, 537 (1956).
- [11] J. W. Darewych, *J. Phys. B: At. Mol. Phys.* **20**, 5925 (1987).
- [12] U. Roy, U. J. Dube, P. Mandal and N. C. Sil, *Comput. Phys. Commun.* **92**, 277 (1995).
- [13] Bransden B H and Joachain C J, *Introduction to Quantum Mechanics* (ELBS/Longman,1989)